

Magnetic particle hyperthermia: nanoparticle magnetism and materials development for cancer therapy

Rudolf Hergt, Silvio Dutz, Robert Müller and Matthias Zeisberger

Institut für Physikalische Hochtechnologie, D-07745 Jena, Germany

E-mail: hergt@ipht-jena.de

Received 5 May 2006, in final form 19 July 2006

Published 8 September 2006

Online at stacks.iop.org/JPhysCM/18/S2919

Abstract

Loss processes in magnetic nanoparticles are discussed with respect to optimization of the specific loss power (SLP) for application in tumour hyperthermia. Several types of magnetic iron oxide nanoparticles representative for different preparation methods (wet chemical precipitation, grinding, bacterial synthesis, magnetic size fractionation) are the subject of a comparative study of structural and magnetic properties. Since the specific loss power useful for hyperthermia is restricted by serious limitations of the alternating field amplitude and frequency, the effects of the latter are investigated experimentally in detail. The dependence of the SLP on the mean particle size is studied over a broad size range from superparamagnetic up to multidomain particles, and guidelines for achieving large SLP under the constraints valid for the field parameters are derived. Particles with the mean size of 18 nm having a narrow size distribution proved particularly useful. In particular, very high heating power may be delivered by bacterial magnetosomes, the best sample of which showed nearly 1 kW g^{-1} at 410 kHz and 10 kA m^{-1} . This value may even be exceeded by metallic magnetic particles, as indicated by measurements on cobalt particles.

1. Introduction

Magnetic nanoparticles being subjected to a magnetic AC field may show remarkable heating effects related to losses during the magnetization reversal process of the particles. The temperature enhancement which occurs in a magnetic nanoparticle (MNP) system under the influence of an external high frequency magnetic field has found applications in techniques (e.g. hardening of adhesives), in chemistry (e.g. thermosensitive polymers, Schmidt 2005) as well as in biomedicine. In the latter case, cancer therapy by hyperthermia (e.g. Gneveckow *et al* 2005, Hilger *et al* 2005), drug targeting via thermosensitive magnetic nanoparticles (Mang 2006) and the application of magnetically controllable catheters (Mohr *et al* 2006) are important

examples. In all cases, it is advantageous to achieve the temperature enhancement needed for a special application with as low as possible amount of MNP. Therefore, the specific loss power (SLP) of the MNP which is measured in watts per gram of magnetic material to be applied must be high enough. This is particularly important for applications where target concentration is very low, for instance in antibody targeting of tumours.

One of the most challenging, until now not satisfactorily solved problems of modern medicine is cancer. Though the standard therapies based on surgery, chemotherapy, irradiation, or combinations of them steadily improve there are many attempts with a multitude of alternative therapy concepts among which different types of hyperthermia have already entered into clinical practice (for a review on hyperthermia in oncology see e.g. Falk and Issels 2001). Besides whole body hyperthermia where the systemic temperature (e.g. by means of a heat bath) has to be carefully controlled to, e.g. 41.8 °C (Robins *et al* 1997), there are different ways of effecting local intracorporal heat generation e.g. by means of microwave radiation, by capacitive or inductive coupling of radiofrequency fields, by implanted electrodes, by ultrasound, or by lasers. Alternatively, in magnetically mediated hyperthermia one deposits magnetic material in the tumour which is heated by means of an external alternating magnetic field. Besides the application of macroscopic magnetic implants ('seeds') which are currently in clinical use for special cancer types, recent studies are focused on magnetic nanoparticles as their heat generation potential appears beneficial and they provide the opportunity of direct tumour targeting through blood circulation (for a review see e.g. Moroz *et al* 2002). Besides the opportunity of a very localized heat generation, the application of magnetic nanoparticles offers the possibility of a self-limitation of the temperature enhancement by using a magnetic material with suitable Curie temperature (e.g. Rand *et al* 1985).

In local hyperthermia, the temperature increase with respect to standard temperature of the human body is considered to be therapeutically useful over a relatively broad temperature range where different mechanisms of cell damaging occur with increasing temperature. Two therapy modalities are commonly differentiated: treatments at temperatures of 42–45 °C for up to few hours—actually denoted as hyperthermia—need a combination with other assisting toxic agents (mostly irradiation or chemotherapy) for reliable damage of tumour cells. In contrast, thermoablation aims for the thermal killing of all tumour cells by applying temperatures in excess of at least 50 °C in the tumour region for exposure times of at least few minutes. Though these short treatment times and the resulting reliable tumour damage look advantageous there are concerns considering critical systemic side effects such as shock syndrome due to sudden release of large amounts of necrotic tumour material and major inflammatory response (Moroz *et al* 2002). In the following, both therapy modalities are comprised as magnetic particle hyperthermia (MPH). In any case, the amount of nanoparticles to be applied should be as small as possible. In order to reach the therapy temperature with minimum particle concentration in tissue the specific heating power of the magnetic nanoparticles in magnetic AC fields should be as high as possible. There is a multitude of known magnetic materials which, however, for biomedical applications is strongly restricted by the demand of biocompatibility. Besides a few suggestions in the literature of using several spinel ferrites or special magnetic alloys for MPH the majority of investigations focused on magnetic iron oxides Fe₃O₄ (magnetite) and γ -Fe₂O₃ (maghemite) which have been proved to be well tolerated by the human body.

Magnetic losses to be utilized for heating arise due to different processes of magnetization reversal in systems of magnetic nanoparticles which depend in different manners on the applied magnetic AC field amplitude and frequency. Moreover, there is a strong dependence of magnetic particle properties on structural ones like mean size, width of size distribution, particle shape and crystallinity. Accordingly, data on specific loss power (SLP) commonly reported in the literature show remarkable scattering of the orders of magnitude of 10–100 W g⁻¹ for a field

amplitude of 10 kA m^{-1} and frequency of about 400 kHz which was suggested to be useful for thermoablation of breast cancer by Hilger *et al* (2005). In early research on magnetic particle hyperthermia either relatively large multidomain particles ($>100 \text{ nm}$, e.g. Gilchrist *et al* 1957) or comparatively small superparamagnetic particles ($<10 \text{ nm}$, e.g. Jordan *et al* 1999) were used. It is shown by the present results that largest values (up to 1 kW g^{-1}) of SLP may be achieved in the transition range from superparamagnetic to stable ferromagnetic properties of the nanoparticles. The reason for the preference of very small MNP in the literature hitherto is mainly due to the fact that in many research labs as well as some firms typical ferrofluids are available which show excellent colloidal stability in the small particle range below about 10 nm.

The goal of the present investigations is to gain deeper insight into the heat generation mechanisms in magnetic nanoparticles over a broad size range from superparamagnetic to stable ferromagnetic particles and to clarify how the particle properties and the electromagnetic field parameters may be optimized for future application in a reliable cancer therapy. Besides the optimization of mean particle diameter and particle size distribution a second route towards larger SLP is expected to be the enhancement of the magnetic moment per particle, e.g. by using Fe or Co particles instead of iron oxides provided that the problem of chemical stability and biocompatibility is satisfactorily solved.

2. Magnetic loss processes

Magnetic losses in an alternating magnetic field to be utilized for heating arise due to different processes of magnetization reversal in the particle system: (1) hysteresis, (2) Néel or Brown relaxation, and (3) frictional losses in viscous suspensions. In comparison to magnetic losses eddy current induced heating of small magnetic particles is negligibly small. The terminus 'inductive heating' occasionally used for magnetic particle heating in biomedical literature is misleading.

2.1. Hysteresis

Hysteresis losses may be determined in a well known manner by integrating the area of hysteresis loops, a measure of energy dissipated per cycle of magnetization reversal (e.g. Bertotti 1998). It depends strongly on the field amplitude as well as the magnetic prehistory. Above a critical particle size domain walls exist and hysteresis losses of those multidomain particles depend in a complicated manner on the type and configuration of wall pinning centres given by the particle structure (for a review see e.g. Kronmüller and Fähnle 2003). For low field amplitudes losses per cycle depend on the field according to a third order power law, commonly denoted as the Rayleigh law, which is theoretically explained by wall pinning. With decreasing particle size a transition to single domain particles occurs, the simplest process of magnetization reversal of which is the uniform mode (Stoner and Wohlfarth 1948). The equilibrium magnetization direction is determined by anisotropy contributions due to crystal structure, particle shape and surface. In the simplest case of uniaxial anisotropy, for an ensemble of randomly oriented, non-interacting, ellipsoidal single domain particles, hysteresis loss energy density is given by twice the anisotropy energy density K . It may be enhanced by nearly a factor of four if particle axes are aligned with the external field. Besides this uniform mode more complicated modes of magnetization reversal (e.g. curling, buckling, fanning) result from micromagnetic theory (e.g. Aharoni 1996). In comparison with the case of uniaxial particles the situation is much more complex for cubic anisotropy. For magnetite particles, Butler and Banerjee (1975) determined theoretically an upper limit of about 80 nm for the single

domain size range which increases considerably with tetragonal particle elongation. The same order of magnitude follows from micromagnetic calculations of Fabian *et al* (1996) considering more sophisticated magnetization patterns like the so-called flower and vortex states. The experimental confirmation of these theoretical models, however, is still open mainly due to the fact that the objects are very small. Recently modern methods of electron microscopy offered possibilities to directly depict the processes of magnetization reversal in individual particles. For instance, the magnetization configuration in bacterial magnetosomes having a mean particle size of about 50 nm was made visible by means of off-axis electron holography by Dunin-Borkowski *et al* (2001). For acicular maghemite particles Eagle and Mallinson (1967) found a strong decrease of coercivity with increasing particle size in the range 30–100 nm which was interpreted as an indication of a non-uniform reversal mode. For magnetite crystals in the mean diameter range above about 50 nm the coercivity and remanence were found to decrease with increasing particle size d according to an empirically well established $d^{-0.6}$ power law (Heider *et al* 1987) which implies a decrease of hysteresis losses in the multidomain size range, too. Since, on the other hand, magnetite particles below about 20 nm become superparamagnetic (see below) a maximum of hysteresis losses may be expected for single domain iron oxide particles near to a mean diameter of 30 nm. Comparing different types of magnetic iron oxide particles (multidomain as well as superparamagnetic one) with respect to their specific loss power (Hergt *et al* 1998) it was shown that hysteresis losses of different types of magnetite particles may differ by orders of magnitude in the range of field amplitudes below 10 kA m^{-1} due to differences of particle size, shape and microstructure.

2.2. Relaxation

With decreasing particle size the energy barrier for magnetization reversal decrease, too, and consequently thermal fluctuations lead to relaxation phenomena. Accordingly, quasistatically measured hysteresis loops (e.g. by VSM) narrow and specific loss power determined thereof becomes smaller than data measured directly by calorimetry. In the case of so-called Néel relaxation (Néel 1949)—i.e. the fluctuation of the magnetic moment direction across an anisotropy barrier—the characteristic relaxation time of a nanoparticle system is given by the ratio of the anisotropy energy KV to the thermal energy kT

$$\tau_N = \tau_0 \exp[KV/(kT)] \quad (\tau_0 \sim 10^{-9} \text{ s}). \quad (1)$$

For a characteristic time of measurement τ_m a critical particle volume V_c may be defined by $\tau_N(V_c) = \tau_m$. For a measuring frequency of 300 kHz and a magnetic anisotropy energy density of 10^4 J m^{-3} (for magnetite particles of ellipsoidal shape with an aspect ratio of 1.4) the critical diameter is about 20 nm. In a fluid suspension of magnetic particles being characterized by a viscosity η , additionally a second relaxation mechanism occurs due to reorientation of the whole particle which is commonly referred to as Brown relaxation with the characteristic relaxation time

$$\tau_B = 4\pi\eta r_h^3/(kT) \quad (2)$$

which was first derived by Debye (1929) for rotational polarization of molecules (r_h is the hydrodynamic radius which due to, e.g., particle coating may be essentially larger than the radius of the magnetic particle core). In the general case, the faster of the relaxation mechanisms is dominant and an effective relaxation time may be defined by

$$\tau_{\text{eff}} = \tau_N \tau_B / (\tau_N + \tau_B). \quad (3)$$

A general treatment of the relaxation in ferrofluids based on a Fokker–Planck equation was given by Shliomis and Stepanov (1994).

The frequency dependence of relaxation of the particle ensemble may be well investigated experimentally by measuring spectra of the complex susceptibility. The imaginary part $\chi''(f)$ which is related to magnetic losses may be described by the well known expression (see e.g. Delaunay *et al* 1995)

$$\chi''(f) = \chi_0 \phi / (1 + \phi^2), \quad \phi = f \tau_{N,B} \quad \chi_0 = \mu_0 M_S^2 V / (kT)$$

(M_S saturation magnetization). (4)

Accordingly, depending on the size distribution width the spectra show more or less pronounced peaks related to Néel or Brown relaxation the position of which is given by $\phi = 1$. Within the validity of linear response theory the loss power density P is related to $\chi''(f)$ according to (e.g. Landau and Lifshitz 1960)

$$P(f, H) = \mu_0 \pi \chi''(f) H^2 f. \quad (5)$$

The loss power density P (W m^{-3}) is related to the specific loss power SLP (W g^{-1}) by the mean mass density of the particles.

According to these equations at low frequencies ($\phi \ll 1$), i.e. in the superparamagnetic regime, losses increase with the square of frequency while for $\phi \gg 1$ losses approach a frequency independent saturation value $P = \mu_0 \pi H^2 (\chi_0 / \tau)$. The strong size dependence of the relaxation times leads to a very sharp maximum of the loss power density in dependence on particle size (Hergt *et al* 1998, 2002). Accordingly, a remarkable output of heating power occurs only for particle systems with narrow size (and anisotropy) distribution with the mean diameter being well adjusted in relation to the treatment frequency. The effect of size distribution on loss power density was elucidated theoretically by Rosensweig (2002).

2.3. Viscous losses

The Brown mechanism causes generation of heat as a result of viscous friction between rotating particles and surrounding medium. This loss type is not restricted to superparamagnetic particles. In general, particles which may be regarded as small permanent magnets with remanent magnetization M_R are subject to a torque moment $T = \mu_0 M_R H V$ when exposed to a rotating magnetic field H . In the steady state the viscous drag in the liquid $12\pi\eta V f$ is counteracted by the magnetic torque T and the loss energy per cycle is simply given by $2\pi T$ (e.g. Hergt and Andrä 2006). The effect of viscous losses was clearly demonstrated in experiments with relatively large (some 100 nm) crushed magnetite particles suspended in an aqueous sol containing commercial gelatine which is stiff below about 30 °C and liquid at higher temperatures (Hiergeist *et al* 1999). On heating above the melting point the specific loss power increases by nearly an order of magnitude up to 200 W g^{-1} at a field amplitude of 6.5 kA m^{-1} and a frequency of 410 kHz.

2.4. Choice of alternating field amplitude and frequency

The above discussion of the different loss mechanism shows that, in principle, specific loss power (SLP) is an increasing function of frequency f and field amplitude H . However, enhancement of SLP by increasing f and H is limited mainly for medical reasons though the realization of large field amplitudes at high frequency in a volume needed for hyperthermia poses a serious technical task, too. In an alternating magnetic field the induction of eddy currents in the patients body may lead to an unwanted heating of both cancerous and healthy tissue reducing in this way the selectivity of the therapy. According to the induction law the induced heating power is proportional to the square of $(H \cdot f \cdot D)$ were H is field amplitude, f frequency and D the induced current loop diameter. A limiting criterion for the product

$H \cdot f$ was experimentally determined by Brezovich (1988) with volunteers. He found for a loop diameter of about 30 cm that a 'test person had a sensation of warmth, but was able to withstand the treatment for more than one hour without major discomfort' if the product $H \cdot f$ was below $4.85 \times 10^8 \text{ A m}^{-1} \text{ s}^{-1}$. For a smaller diameter of the body region being exposed to the alternating magnetic field, e.g. in the case of breast cancer, and depending on the seriousness of the illness this critical product may be exceeded. For instance, for the first commercially developed equipment for treatment of human patients a frequency of 100 kHz and a field amplitude up to 18 kA m^{-1} was reported (Gneveckow *et al* 2004). The different dependences of SLP on field parameters for different loss types discussed above show that the combination of AC field amplitude and frequency is to be favourably chosen depending on the type of particles to be used for the therapy. For particles with mean size in the superparamagnetic regime losses increase with frequency according to equation (5) taking into account the non-linear frequency dependence of the imaginary part of the susceptibility (equation (4)). In contrast, the dependence of hysteresis losses on frequency is linear for ferromagnetic particles. The dependence of magnetic losses on field amplitude obeys a square law for superparamagnetic particles (cf equation (5)) while for larger ferromagnetic particles in the Rayleigh regime a third order power law is valid. As a consequence, for instance, for particles with hysteresis losses within the validity range of the Rayleigh regime one should favour the field amplitude against frequency in the limiting product $H \cdot f$. In contrast, for superparamagnetic particles frequency has to be overweighted against field amplitude. The experimental results presented below will give a contribution to elucidating the relation of specific loss power with structural particle properties (mainly size) on one hand and alternating field parameters on the other in the framework of above sketched loss mechanisms.

3. Specific loss power of different classes of iron oxide particles

At present, a variety of approved types of magnetic iron oxide particles for specific contrast enhancement in nuclear magnetic resonance imaging (MRI) are available on the market. However, these relatively small, superparamagnetic particles are not well suited for MPH due to insufficient heating power as shown, for instance, for Endorem[®] by Hergt *et al* (1998). Though a broad spectrum of preparation methods for nanoparticles was developed in the literature, guidelines for the preparation of particles with optimum magnetic properties for MPH have not been known until now. In the present investigations besides own products some promising particle types from different manufacturers and research groups were selected for checking their value with respect to requirements for magnetic particle hyperthermia.

3.1. Superparamagnetic particles

Superparamagnetic particles were tested by several authors for hyperthermia applications whereas the particle types used differed considerably with respect to their specific loss power (SLP) (Andrä 1998). Though a direct comparison of SLP data measured at different field parameters is problematic, in summary most values are more or less unsatisfactory as discussed in detail recently by Hergt and Andrä (2006). Therefore, in the present investigations some special magnetic colloidal suspensions were investigated which showed large values of SLP.

3.1.1. Size fractionated aqueous suspensions of maghemite. As an example of commercial ferrofluids the aqueous iron oxide suspension DDM 128N 1020 (Meito Sangyo, Japan) was investigated which is used as raw material for the MRI contrast agent Resovist[®]. The ferrimagnetic cores which were shown to consist of maghemite ($\gamma\text{-Fe}_2\text{O}_3$) by means of x-ray diffraction (XRD) are covered by carboxydextran (MW 2600 Da). Investigation of

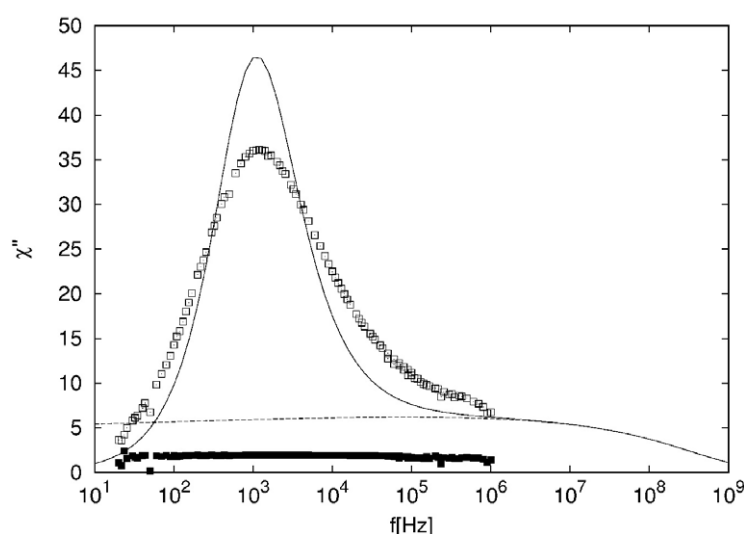


Figure 1. Experimental frequency spectrum of the imaginary part of the susceptibility for a colloidal suspension of maghemite particles (open symbols) and the same particles immobilized in mannitol (full symbols) in comparison to results of relaxation theory (full and dashed line; cf the text).

the size distribution by means of different methods (transmission electron microscopy (TEM), atomic force microscopy (AFM) as well magnetic analysis after Chantrell *et al* (1978)) made clear that the original ferrofluid covered a broad size range of about 5–20 nm. To elucidate the influence of particle size on SLP the original ferrofluid was subjected to a magnetic fractionation procedure which is described in detail in a separate paper (Glöckl *et al* 2006). The mean particle diameter of the fractions gained varied between about 6 and 20 nm. All fractions consist of typical superparamagnetic particles obeying the Langevin theory in quasistatic magnetization measurements. Experimental coercivity data are extremely small in comparison to the anisotropy field of ellipsoidal single domain maghemite particles. In order to check the validity of the above discussed relaxation theory spectra of the complex susceptibility were measured by means of AC susceptometry as described previously (Hergt *et al* 2004a). For discrimination of Néel and Brown relaxation, particles were immobilized by freeze-drying the suspensions after addition of 5 vol% mannitol. For both the liquid as well as immobilized fractions, frequency spectra of the SLP were derived from the imaginary part of the susceptibility according to equation (5). The results were checked by direct calorimetric determination of SLP at large field amplitude of 8 kA m^{-1} and frequencies of 100–400 kHz.

While frequency spectra of common ferrofluids due to a broad size distribution are rather flat, the gained fractions exhibit clear peaks which could be shown to be related to Brown relaxation. As a typical example figure 1 shows the frequency spectrum of the imaginary part of the susceptibility for the largest diameter fraction (about 18 nm after the Chantrell method). The data points shown represent experimental results for the fluid suspension (open symbols) as well as immobilized particles (full symbols). On comparing the two spectra the effect of Brown relaxation becomes obvious. The low frequency peak of χ'' found for the liquid suspension vanishes after immobilizing the particles. From the peak position a mean hydrodynamic diameter of 73 nm may be derived using equation (2). It is in good accordance with the value of 69 nm determined by photon correlation spectroscopy (Glöckl *et al* 2006). The experimental results could be theoretically well explained by introducing

the experimentally determined log-normal size distribution into the above discussed model of combined Néel and Brown relaxation. As the result, figure 1 shows the theoretical spectrum of the fluid suspension (full line) and of the immobilized particles (dashed line). Parameters entering the calculations are, besides the constants of the experimentally determined log-normal distribution, the magnetization of maghemite (410 kA m^{-1}), an anisotropy energy density of 15 kJ m^{-3} and a hydrodynamic diameter of three times the core diameter. For the fluid the viscosity of water and for the immobilized particles an effective viscosity of 10^3 Pa s (which is equivalent to nearly complete elimination of Brown relaxation) was used. Considering that no other free parameters entered the model, the description of the shape of the spectra and the right order of magnitude of the absolute values of susceptibility is satisfactory. Since the imaginary part of the susceptibility represents magnetic losses the vanishing of the Brown relaxation peak after immobilization implies a considerable reduction of specific heating power in hyperthermia, e.g. when particles circulating in blood start sticking on tumour cells or enter into the cell plasma. It could be shown that a derivation of the specific loss power from the imaginary part of the susceptibility by using the linear response theory (equations (1)–(5)) agreed well with data determined calorimetrically for a high field amplitude of 11 kA m^{-1} . At this field amplitude and a frequency of 410 kHz a value of 400 W g^{-1} resulted for the largest size fraction (mean size 18 nm). With decreasing mean size of the particle fractions the SLP decreases rapidly (Hergt *et al* 2004b).

3.1.2. Ferrofluid with normal size distribution. As another representative example a special ferrofluid of dextran covered maghemite was investigated which distinguished itself by showing nearly a normal size distribution instead of the commonly found log-normal one (Hergt *et al* 2004a). Introducing the experimental size distribution (determined from TEM images) into the relaxation model as described above again resulted in a very satisfactory description of susceptibility spectra. For these particles with a mean core size of 15 nm a specific loss power of the order of 600 W g^{-1} at a field amplitude of 11 kA m^{-1} and a frequency of 400 kHz were found; this is an appreciable value in comparison to common ferrofluids known until now.

Looking for decisive parameters for the amount of loss power the mean particle size (in combination with narrow size distribution) was found to be most important. It could be shown that in the superparamagnetic size range (up to about 20 nm for maghemite) SLP is a steeply increasing function with increasing core size (Hergt and Andrä 2006). Since one may anticipate that this increase continues into the stable single domain size range before at larger diameters a decrease of SLP for multidomain particles occurs, investigations were extended to the particle size range $20\text{--}50 \text{ nm}$.

3.2. Iron oxide nanoparticles in the single domain size range

While superparamagnetic particles are readily available from a number of different manufacturers, there are only a few sources for iron oxide particles in the diameter range of $20\text{--}50 \text{ nm}$. One exceptional method of preparation of such magnetic iron oxide particles was developed by nature: synthesis by magnetotactic bacteria.

3.2.1. Bacterial magnetosomes. The synthesis of magnetosomes by magnetotactic bacteria and their main properties are the subject of several review papers given in the literature (e.g. Philipse and Maas 2002, Heyen and Schüler 2003). Magnetosomes prepared by the group of Schüler in a range of mean size of $30\text{--}40 \text{ nm}$ with a mean square deviation of 5 nm were investigated by the present authors with respect to specific loss power. Since in this diameter range remarkable hysteresis occurs losses were determined by three different

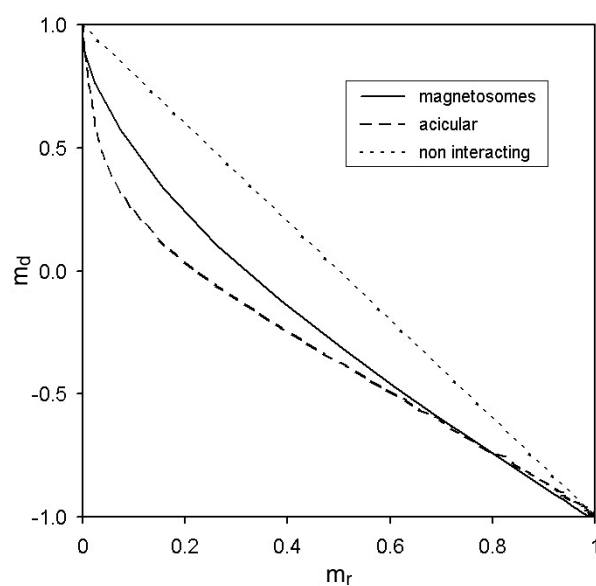


Figure 2. Henkel plot of bacterial magnetosomes in comparison to an acicular particle powder for recording applications.

methods: extrapolation from imaginary part of susceptibility—as described above—and integration of hysteresis loops measured by vibrating sample magnetometry (VSM) and also direct calorimetric measurements at fixed field of 10 kA m^{-1} and a frequency of 410 kHz (Hergt *et al* 2005). In summary, the first two methods gave underestimations of SLP compared to calorimetric results. Extrapolation from AC susceptibility spectra failed since the square law of field dependence supposed in the linear response model (equation (4)) could not be confirmed experimentally. Instead a change from square law to a third order power above a field amplitude of 2 kA m^{-1} was observed. On the other hand, hysteresis losses are measured to be so small since relaxation effects during the comparatively slow VSM measurement cannot be ruled out. The calorimetric measurement resulted in a value of 960 W g^{-1} for the best sample at the above given field parameters.

For elucidation of the role of magnetic interaction within the chains which magnetosomal particles form so-called Henkel plots (see e.g. Bertotti 1998) were measured. Figure 2 shows the results for magnetosomes in comparison with a sample of acicular maghemite particles commonly used in recording industry. The deviations from the linear dependence predicted for a non-interacting particle ensemble are clearly seen for magnetosomes though not so pronounced as for acicular particles which will be discussed below.

Though the measured specific loss power of magnetosomes is appealing, the applicability of these bacterial iron oxide particles is restricted due to their complicated synthesis, as well as some medical reservation considering the bacterial protein coating. Therefore a study was started to investigate magnetic losses in nanoparticles prepared by wet chemical precipitation in a broad size range from about 10 nm up to 100 nm covering the transition from superparamagnetism via single domain to multidomain particles.

3.2.2. Wet chemically precipitated single domain particles. There is a manifold of different preparation methods for magnetic nanoparticles a review of which was recently given by

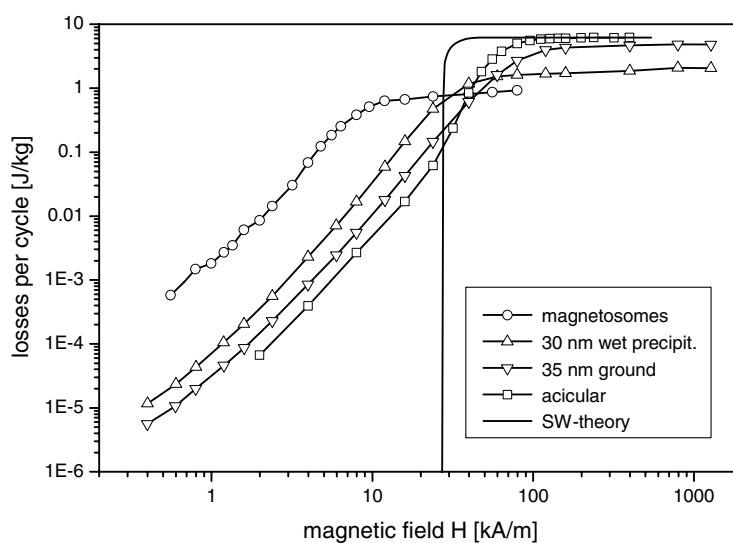


Figure 3. Dependence of losses per cycle on minor loop field amplitude for magnetic nanoparticles prepared in different way (cf the text) in comparison with Stoner–Wohlfarth theory (full line).

Tartaj *et al* (2003). The most common preparation method for iron oxides is wet chemical precipitation. In general, an aqueous solution of a mixture of a ferrous and a ferric salt is reacting with a basic medium ($\text{pH} > 8$). Mean particle size may be well controlled for typical superparamagnetic particles (~ 10 nm diameter) as documented often in the literature. However, growing particles to larger mean diameter commonly results in a very broad size distribution and problems with particle agglomeration occur. There are serious difficulties in preparing stable aqueous suspensions with mean diameter above about 20 nm. In a separate study (Dutz *et al* 2005) magnetic iron oxide particles were prepared by two different wet chemical methods in comparison to grinding larger commercial magnetite particles. In the first step, particle powders covering a mean size range (determined by XRD) of about 15 nm up to 100 nm were investigated, details of which were described previously (Dutz *et al* 2006b). In summary, magnetic properties show a well defined systematic dependence on mean particle size but differ essentially from magnetosomes. For illustration, figure 3 shows the dependence of hysteresis losses per cycle on field amplitude of minor loops for selected samples of similar mean size of about 35 nm. For comparing precipitation with grinding a typical sample of mean size of 30 nm prepared wet chemically and a sample prepared by grinding of a commercial magnetite powder of starting size of about 300 nm for 24 h down to 35 nm are shown. In addition, as cornerstones the results for magnetosomes (35 nm mean diameter) and a typical acicular maghemite powder for recording (about $50 \text{ nm} \times 500 \text{ nm}$, Hergt *et al* 1998) are presented. Further, for comparison with the experimental data a theoretical curve for a Stoner–Wohlfarth (SW) system fitted to the saturation of the recording material is shown. Saturation losses decrease in the order: acicular—ground—wet chemical—bacterial particles, in clear correlation with the coercivity of the samples. The maximum loss per cycle of the acicular particles of 7 J kg^{-1} would deliver an enormous specific heating power of 2.8 kW g^{-1} at 400 kHz. However, with a field amplitude of 100 kA m^{-1} needed for a saturation hysteresis loop the above given criteria for avoidance of health damage of the patient ($H \cdot f < 5 \times 10^8 \text{ A m}^{-1} \text{ s}^{-1}$) would be violated. On the other hand, a reduction of frequency to 5 kHz demanded by the above criteria would reduce heating power to meagre 35 W g^{-1} .

This example shows that a low coercivity is favourable for particles designed for hyperthermia. Comparing all samples shown in figure 3 with respect to this issue and considering the above reported data for magnetosomes the outstanding properties of the latter become clear. In particular relatively large losses are generated already with low field amplitudes below 10 kA m^{-1} . Such a field amplitude is, for instance, the maximum value achieved with a $15 \text{ kW}/400 \text{ kHz}$ AC generator and a coil for treatment of breast cancer (Hilger *et al* 2005).

Remarkably, none of the experimental data follow the SW model. There is a principal difference at low field amplitudes: while the SW model predicts a threshold field for hysteresis losses the experimental results for all investigated particle types show power laws with the power varying from two to three. The latter is valid for the so-called Rayleigh losses (e.g. Kronmüller and Fähnle 2003). Three main reasons may be anticipated for the deviation of experimental results from standard theory at least for the technically produced particles. Firstly, particles have a broad size distribution and accordingly the deviation may be caused by a fraction of large diameter particles. Secondly, in powders magnetic dipolar interactions may be important. Third, the SW model holds for ellipsoidal particles with uniaxial anisotropy while one deals in the present case with non-ellipsoidal particles of cubic crystal symmetry. At least the first reason rarely applies to bacterial magnetosomes the iron oxide particles of which have a narrow size distribution. Moreover, if the low field power law is caused by a large diameter fraction, the weight of this fraction (i.e. the Rayleigh factor of the power law) should increase with increasing mean size. This is in contradiction to the experimental results. Regarding the second reason, dipolar interaction within the linear chains of magnetosomes may be possible as indicated by the above presented results of Henkel plots (figure 2) and as shown by imaging of the particle fields by Dunin-Borkowski *et al* (2001). The resulting stray field is quite different from what is expected for an arrangement of particles in a spherical cluster. In the latter case, the geometrical configuration of particles allows for a variety of closed loop arrangements of particle moments, quite different from the linear chain configuration. As an experimental confirmation, the observed relative saturation remanence for magnetosomes has a value of 0.27 in contrast to 0.18 for precipitated as well as ground powders. In the Henkel plot the curves of the latter are positioned between magnetosomes and acicular particles shown in figure 2.

In order to reduce the particle clustering which occurs in powders, particles were coated immediately after precipitation in aqueous suspension by carboxymethyl dextran (CMD), details of which will be described elsewhere (Dutz *et al* 2006a). As a typical result, figure 4 shows the field dependence of losses per cycle for CMD-stabilized aqueous fluids in comparison to data for magnetosomes. The effect of mean particle core diameter determined using XRD is clearly visible: for low field amplitudes losses increase with decreasing mean particle size. In comparison to the case for uncoated particles, for powders the curves of CMD-stabilized fluids measured for corresponding mean particle sizes are shifted towards the data for magnetosomes.

As a typical example of the structure of the CMD-stabilized particles figure 5 shows a transmission electron micrograph of one of the samples the results of which are shown in figure 4. Obviously, there are spherical clusters of mean diameter of about 60 nm showing small nuclei in the centre covered by larger grains of about 18 nm diameter. From XRD line broadening a mean diameter of 17 nm is found for this sample. This result shows that the grains of the clusters are crystallographically non-coherent which is confirmed by diffraction features in TEM images. Cluster size is reduced by the stabilization procedure in comparison to that for powders where a mean cluster diameter of about 80 nm may be deduced from scanning electron images (Dutz *et al* 2006b). There are indications from TEM imaging that the CMD coating covers not individual grains but clusters. This means that clustering occurs in a relatively early stage of particle growth before the coating process is effective.

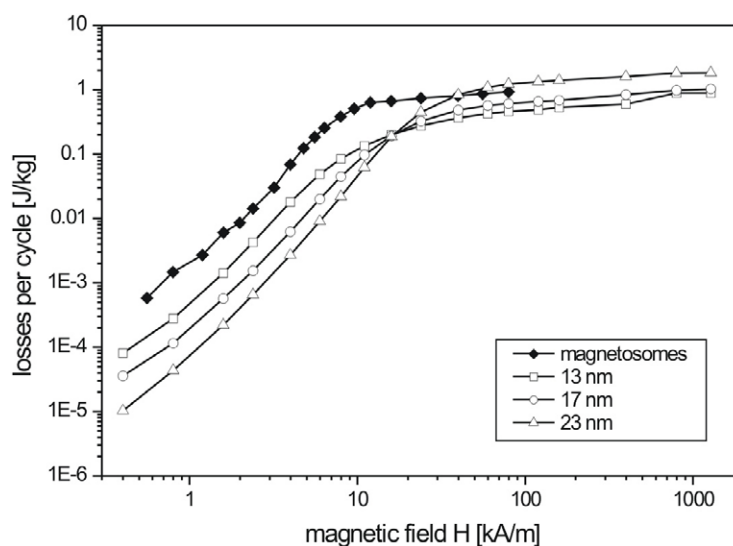


Figure 4. Dependence of losses per cycle on the field amplitude for CMD-stabilized aqueous fluids of different mean particle core diameter determined by XRD in comparison to data for magnetosomes.

For avoiding this the precipitation conditions must be experimentally refined to allow a better control of the nucleation stage of the particles. One basic way towards preparing relatively large particles with narrow size distribution is the separation of the nucleation stage from further particle growth. Successful control of the quantity of nanoparticle seeds with resulting well defined particle diameters is reported by Sun and Zeng (2002). An alternative method for growing particles comparatively slowly is the glass crystallization method. The method which proved good for Ba ferrite particles was recently used to prepare γ -Fe₂O₃ nanopowders, too (Müller *et al* 2005, 2006). The mean particle size may be controlled by the parameters of the annealing procedure. Nevertheless, further systematic investigations for optimizing preparation procedures are necessary in order to provide nanoparticles with tailored magnetic properties.

3.3. Metallic magnetic particles

The results for magnetic iron oxide nanoparticles presented above have shown which limitations for the specific loss power (SLP) of this substance class may be expected. An alternative route towards larger SLP is the application of particle types with larger magnetization, e.g. by using metallic iron or cobalt or alloys thereof. Drawbacks of metallic particles in comparison to the iron oxides are lower chemical stability and reduced biocompatibility. The preparation of metallic nanoparticles and stable colloidal suspensions thereof in organic fluid were reported by different groups for Co (e.g. Bönnemann *et al* 2003, Zhang *et al* 2003, Wagener *et al* 1999), Fe (Mendoza-Reséndez *et al* 2004), and FeCo (Hütten *et al* 2005).

Presently, cobalt nanoparticles prepared by thermolysis of Co₂(CO)₈ by the group of Bönnemann were investigated with respect of specific loss power in comparison to the above described iron oxide particle types. Preparation conditions were described in detail elsewhere. (Bönnemann *et al* 2003). Shortly, after synthesis particles were either dried *in vacuo* to prepare a dry powder or were coated with Korantin SH and peptized in kerosene in order to get an

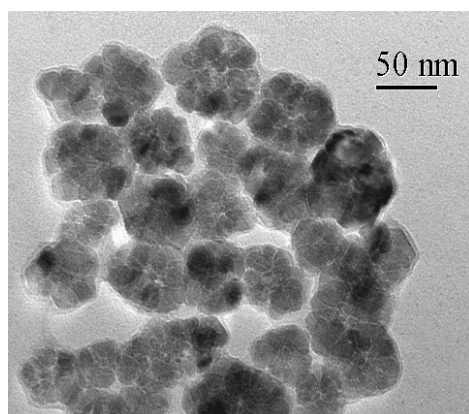


Figure 5. TEM image of CMD-coated iron oxide particles prepared by wet chemical precipitation. (Courtesy C Oestreich, Institute of Ceramic Materials, Freiberg University of Mining and Technology.)

air stable magnetic fluid. Samples of the dry powder as well as suspensions in kerosene were investigated in the present paper. XRD shows that particles are mainly fcc cobalt with a small amount of Co_3O_4 supposedly as the coating of the metallic core. From the diffraction linewidth of the $\text{Co}(111)$ peak one estimates a mean core diameter of 6 nm. By TEM imaging a mean diameter of 9 nm was found. An effective hydrodynamic diameter of 26 nm was derived from the position of the Brown peak in AC susceptibility spectra. From magnetization measurements a specific magnetization of 77.5 emu g^{-1} is found for the powder sample. This value is only 46% of the bulk value of 168 emu g^{-1} for (hex) cobalt. Assuming that particles consist of a cobalt core and a coating of some non-magnetic or weakly magnetic material of mean density of 5 g cm^{-3} one estimates a mean thickness of this layer to be about 0.7 times the core diameter. Magnetic properties of Co nanoparticles were investigated in the same way as described above for iron oxide particles. A rather large value of the measured DC susceptibility of 220 indicates large magnetic losses in the framework of the above discussed relaxation theory. Magnetization loops show a hysteresis with a coercivity of 6.4 kA m^{-1} for the saturation loop. To avoid problems with the determination of specific loss power either by extrapolation from relaxation theory or from the hysteresis loop area discussed above, the specific loss power of the suspension was measured calorimetrically for a field amplitude of 10 kA m^{-1} at 410 kHz. The value found, 720 W g^{-1} , is larger than all data reported above for magnetic iron oxides with exception of the bacterial magnetosomes. Considering that particles were not optimized yet with respect to large SLP (e.g. by composition, mean size, size distribution width) one may expect future values beyond 1 kW g^{-1} . However, for application in hyperthermia the problem of stable aqueous suspensions of metallic particles will have to be solved.

4. Conclusions

It follows from the discussion of the above presented experimental results in the framework of common models of loss mechanisms that the specific loss powers of different types of magnetic nanoparticles may differ by orders of magnitude. The most important parameter is the mean particle size in combination with a narrow size distribution. For superparamagnetic particles a steep decline of SLP with decreasing particle size is found. Commercially readily available, very small superparamagnetic particles (below about 10 nm mean diameter) are not

the optimum choice for effective tumour heating. By analysis of the heat balance of a tumour in body tissue, relations between SLP, particle concentration in the tumour and tumour diameter were derived recently (cf Hergt and Andrä 2006). As a result, the demand for SLP increases with an inverse second order power law with decreasing tumour size. Considering common values of specific heating power reported in the literature (some tens of W g^{-1}) combined with currently preferred particle concentrations of about 10 mg cm^{-3} for intratumoural injection, it was shown that the diameter of the heated tissue region must not be smaller than 1 cm even if the tumour is considerably smaller. For the low particle concentrations of magnetic material transported by antibody targeting into the tumour region a useful effect may be expected only for even (much) larger tumours if the specific loss power is not increased by orders of magnitude. In particular, a significant temperature increase for isolated tumour cells filled by magnetic particles ('intracellular hyperthermia', e.g. Jordan *et al* 1999) cannot be expected, as was already estimated by Rabin (2002). In the present investigations, large values of SLP of the order of some hundreds of W g^{-1} at 400 kHz and 10 kA m^{-1} are found for particles with mean size of about 18 nm provided that the size distribution is sufficiently narrowed by means of magnetic fractionation or by a well controlled preparation technique. A very large value of SLP of nearly 1 kW g^{-1} is found for bacterial magnetosomes having a mean diameter of the magnetite crystals of about 35 nm. However, since the productivity of bacteria is rather low and there are concerns regarding biocompatibility of the bacterial protein coating, the technical preparation of stable suspensions of magnetic single domain particles is highly desirable. The present results show considerable differences of magnetic properties of magnetosomes and technically prepared particles of comparable size which are hardly explicable within present micromagnetic models of single domain particles. Reasons may be a broad size distribution, complicated anisotropy (e.g. cubic) and shape (polyhedral) of the particles. Here, further elucidation of structural properties of the particle ensemble in relation to coercivity, remanence and magnetic losses is necessary. For better defined particle properties precipitation conditions must be experimentally refined to allow a better control of the nucleation stage of the particles. In particular, a separation of the nucleation stage from further particle growth seems to be favourable for preparing single domain particles with narrow size distribution. As an important issue, clustering of particles has to be further reduced by improved *in situ* coating of the nuclei from the beginning of precipitation. As an alternative to magnetic iron oxides, magnetic metallic particles (in particular iron) offer the possibility of increased SLP as may be concluded from the above described first experiments with cobalt nanoparticles. Values of SLP of some kW g^{-1} at the typical alternating field amplitude of 10 kA m^{-1} and a frequency of 500 kHz seem to be realistic.

Acknowledgments

The authors gratefully acknowledge financial support by the Deutsche Forschungsgemeinschaft, SPP 1104, contract HE 2878/9. They thank Dr C Oestreich, Institute of Ceramic Materials, Freiberg University of Mining and Technology for TEM imaging as well as all partners from the DFG-priority programme 'Colloidal magnetic fluids' (SPP 1104) for good cooperation.

References

- Aharoni A 1996 *Introduction to the Theory of Ferromagnetism* (Oxford: Clarendon)
- Andrä W 1998 Magnetic hyperthermia *Magnetism in Medicine* ed W Andrä and H Nowak (Berlin: Wiley-VCH) pp 455–70

- Bertotti G 1998 *Hysteresis in Magnetism* (London: Academic)
- Bönnemann H, Brijoux W, Brinkmann R, Matoussevitch N, Waldöfner N, Palina N and Modrow H 2003 A size-selective synthesis of air stable colloidal magnetic cobalt nanoparticles *Inorg. Chim. Acta* **350** 617–24
- Brezovich I A 1988 Low frequency hyperthermia *Med. Phys. Monograph* **16** 82–111
- Butler R F and Banerjee S K 1975 Theoretical single-domain grain size range in magnetite and titanomagnetite *J. Geophys. Res.* **80** 4049–58
- Chantrell R W, Popplewell J and Charles S W 1978 Measurements of particle size distribution parameters in ferrofluids *IEEE Trans. Magn.* **14** 975
- Debye P 1929 *Polar Molecules* (New York: Dover)
- Delaunay L, Neveu S, Noyel G and Monin J 1995 A new spectrometric method using magneto-optical effect to study magnetic liquids *J. Magn. Magn. Mater.* **149** L239–49
- Dunin-Borkowski R E, McCartney M R, Pósfai M, Frankel R B, Bazylinski D A and Buseck P R 2001 Off-axis electron holography of magnetotactic bacteria: magnetic microstructure of strains MV-1 and MS-1 *Eur. J. Mineral.* **13** 671
- Dutz S, Andrä W, Hergt R, Müller R, Oestreich Ch, Schmidt Ch, Töpfer J, Zeisberger M and Bellemann M 2006a Influence of dextran coating on the magnetic behavior of iron oxide nanoparticles, at press
- Dutz S, Hergt R, Mürbe J, Müller R, Zeisberger M, Andrä W, Töpfer J and Bellemann M E 2006b Hysteresis losses of magnetic nanoparticle powders in the single domain size range *J. Magn. Magn. Mater.* at press
- Dutz S, Hergt R, Mürbe J, Töpfer J, Müller R, Zeisberger M, Andrä W and Bellemann M E 2005 Magnetic nanoparticles for biomedical heating applications *Z. Phys. Chem.* **220** 145–51
- Eagle D F and Mallinson J C 1967 On the coercivity of γ -Fe₂O₃ particles *J. Appl. Phys.* **38** 995–7
- Fabian K, Kirchner A, Williams W, Heider F, Leibl F and Hubert A 1996 Three-dimensional micromagnetic calculations for magnetite using FFT *Geophys. J. Int.* **124** 89–104
- Falk M H and Issels R D 2001 Hyperthermia in oncology *Int. J. Hyperthermia* **17** 1
- Gilchrist R K, Medal R, Shorey W D, Hanselman R C, Parrot J C and Taylor C B 1957 Selective inductive heating of lymph nodes *Ann. Surg.* **146** 596
- Glöckl G, Hergt R, Zeisberger M, Dutz S, Nagel S and Weitschies W 2006 Effect of field parameters, nanoparticle properties and immobilization on the specific heating power in magnetic particle hyperthermia *J. Phys.: Condens. Matter* **18** S2935–49
- Gneveckow U *et al* 2004 Description and characterization of the novel hyperthermia- and thermoablation system *Med. Phys.* **31** 1444–51
- Gneveckow U *et al* 2005 Magnetic force nanotherapy *Biomed. Tech.* **50** 92–3
- Heider F, Dunlop D J and Sugiura N 1987 Magnetic properties of hydrothermally recrystallized magnetite crystals *Science* **236** 1287–90
- Hergt R and Andrä W 2006 Magnetic hyperthermia and thermoablation *Magnetism in Medicine* 2nd ed ed W Andrä and H Nowak (Berlin: Wiley–VCH)
- Hergt R, Andrä W, d'Ámbly C G, Hilger I, Kaiser W A, Richter U and Schmidt H G 1998 Physical limits of hyperthermia using magnetite fine particles *IEEE Trans. Magn.* **34** 3745–54
- Hergt R, Hiergeist R, Hilger I and Kaiser W A 2002 Magnetic nanoparticles for thermoablation *Recent Res. Dev. Mater. Sci.* **3** 723–42
- Hergt R, Hiergeist R, Hilger I, Kaiser W A, Lapatinikov Y, Margel S and Richter U 2004a Maghemite nanoparticles with very high AC-losses for application in RF-magnetic hyperthermia *J. Magn. Magn. Mater.* **270** 345–57
- Hergt R, Hiergeist R, Zeisberger M, Glöckl G, Weitschies W, Ramirez L P, Hilger I and Kaiser W A 2004b Enhancement of AC-losses of magnetic nanoparticles for heating applications *J. Magn. Magn. Mater.* **280** 358–68
- Hergt R, Hiergeist R, Zeisberger M, Schüler D, Heyen U, Hilger I and Kaiser W A 2005 Magnetic properties of bacterial magnetosomes as potential diagnostic and therapeutic tools *J. Magn. Magn. Mater.* **293** 80–6
- Heyen U and Schüler D 2003 Growth and magnetosome formation by microaerophilic magnetospirillum strains in an oxygen-controlled fermentor *Appl. Microbiol. Biotechnol.* **61** 536–44
- Hiergeist R, Andrä W, Buske N, Hergt R, Hilger I, Richter U and Kaiser W A 1999 Application of magnetite ferrofluids for hyperthermia *J. Magn. Magn. Mater.* **201** 420–2
- Hilger I, Hergt R and Kaiser W A 2005 Use of magnetic nanoparticle heating in the treatment of breast cancer *IEE Proc. Nanobiotechnol.* **152** 33–9
- Hütten A, Sudfeld D, Ennen I, Reiss G, Wojczykowski K and Jutzi P 2005 Ferromagnetic FeCo nanoparticles for biotechnology *J. Magn. Magn. Mater.* **293** 93–101
- Jordan A, Scholz R, Wust P, Schirra H, Schiestel T, Schmidt H and Felix R 1999 Endocytosis of dextran and silan-coated magnetite nanoparticles and the effect of intracellular hyperthermia on human mammary carcinoma cells *in vitro J. Magn. Magn. Mater.* **194** 185–96

- Kronmüller H and Fähnle M 2003 *Micromagnetism and the Microstructure of Ferromagnetic Solids* (Cambridge: Cambridge University Press)
- Landau L D and Lifshitz E M 1960 *Electrodynamics of Continuous Media* (London: Pergamon)
- Mang T 2006 Steuerbare Nanopartikel für schonende Chemotherapie *Presse-Mitteilung* <http://idw-online.de/pages/de/news149649>
- Mendoza-Reséndez R, Bomati-Miguel O, Morales M P, Bonville P and Serna C J 2004 Microstructural characterization of ellipsoidal iron metal nanoparticles *Nanotechnology* **15** S254–8
- Mohr R, Kratz K, Weigel T, Lucka-Gabor M, Moneke M and Lendlein A 2006 Initiation of shape-memory effect by inductive heating of magnetic nanoparticles in thermoplastic polymers *Proc. Natl Acad. Sci.* **103** 3540–5
- Moroz P, Jones S K and Gray B N 2002 Magnetically mediated hyperthermia: current status and future directions *Int. J. Hyperthermia* **18** 267–84
- Müller R, Hergt R, Dutz S, Zeisberger M and Gawalek W 2006 Nanocrystalline iron oxide and Ba-ferrite particles in the transition range superparamagnetism–ferromagnetism for ferrofluid applications *J. Phys.: Condens. Matter* **18** S2527–42
- Müller R, Hergt R, Zeisberger M and Gawalek W 2005 Preparation of magnetic nanoparticles with large specific loss power for heating applications *J. Magn. Magn. Mater.* **289** 13–6
- Néel L 1949 Influence des fluctuations thermiques a l'aimantation des particules ferromagnétiques *C. R. Acad. Sci.* **228** 664–8
- Philipse A P and Maas D 2002 Magnetic colloids from magnetotactic bacteria: chain formation and colloidal stability *Langmuir* **18** 9977–84
- Rabin Y 2002 Is intracellular hyperthermia superior to extracellular hyperthermia in the thermal sense *Int. J. Hyperthermia* **18** 194–9
- Rand R W, Snow H D, Elliott D G and Haskins G M 1985 Induction heating method for use in causing necrosis of neoplasm *US Patent Specification* 4,545,368
- Robins H I *et al* 1997 Phase I clinical trial of melphalan and 41.8 °C whole-body hyperthermia in cancer patients *J. Clin. Oncol.* **15** 158
- Rosensweig R E 2002 Heating magnetic fluid with alternating magnetic field *J. Magn. Magn. Mater.* **252** 370–4
- Schmidt A M 2005 Induction heating of novel thermoresponsive ferrofluids *J. Magn. Magn. Mater.* **289C** 5–8
- Shliomis M I and Stepanov V I 1994 Theory of dynamic susceptibility of magnetic fluids *Relaxation Phenomena in Condensed Matter* ed W Coffey (Chichester: Wiley)
- Stoner E C and Wohlfarth E P 1948 A mechanism of magnetic hysteresis in heterogeneous alloys *Phil. Trans. R. Soc. A* **240** 599–642
- Sun S and Zeng H 2002 Size controlled synthesis of magnetite nanoparticles *J. Am. Chem. Soc.* **124** 8204–5
- Tartaj P, del Puerto-Morales M, Veintemillas-Verdaguer S, Gonzalez-Carreno T and Serna C J 2003 The preparation of magnetic nanoparticles for applications in biomedicine *J. Phys. D: Appl. Phys.* **36** R182–97
- Wagener M, Günther B and Blums E 1999 Preparation of oxidation resistant cobalt oil colloids *J. Magn. Magn. Mater.* **201** 18–22
- Zhang X X, Wen G H, Xiao G and Sun S 2003 Magnetic relaxation of diluted and self-assembled cobalt nanocrystals *J. Magn. Magn. Mater.* **261** 21–8